IEEE Access
The journal for rapid open access publishing

Received June 24, 2015, accepted July 6, 2015, date of publication July 10, 2015, date of current version July 22, 2015.

Digital Object Identifier 10.1109/ACCESS.2015.2454295

An Investigation of Earth Grid Performance Using Graphene-Coated Copper

AMIT JYOTI DATTA[1], (Student Member, IEEE), RICHARD TAYLOR[1], (Member, IEEE), GEOFFREY WILL[2], AND GERARD LEDWICH[1], (Senior Member, IEEE)
[1]School of Electrical Engineering and Computer Science, Queensland University of Technology, Brisbane, QLD 4000, Australia
[2]School of Chemistry Physics and Mechanical Engineering, Queensland University of Technology, Brisbane, QLD 4000, Australia

Corresponding author: A. J. Datta (amit.jyoti.datta@gmail.com)

This work was supported by Powerlink Queensland, Virginia, QLD, Australia.

ABSTRACT Large power systems are normally operated with their neutral points directly earthed. At a major generating or switching station, this results in the provision of a large earth grid buried in the ground. The design of earthing systems requires a worst case approach. There is a possibility of heavy currents flowing into the earth grid from the overhead earth wires through the tower during a line conductor fault and from lightning strikes. The flow of earth current during a fault or lightning conditions results in a rise of earth grid potential with respect to a physically remote earth point, which can lead to unsafe conditions under some conditions for personnel and connected electrical plant. This paper aims to investigate the potential of adding novel coatings to the conventional copper earth grid conductors to enhance overall conductivity and diminish corrosion. This contributes to lowering the rise of earth grid potential. Graphene-coated copper performance as an earth grid conductor is evaluated with staged low voltage fault and the corrosion behavior in both a destructive and nondestructive environment. A comparison of the simulation software packages CDEGS and CST is also carried out using lightning strike conditions.

INDEX TERMS Earth grid, graphene, tube furnace, scanning electron microscopy, Raman microscopy, electrochemical impedance spectroscopy, Nyquist plot, bode plot, soil resistivity, electric field, impedance matching.

I. INTRODUCTION

In general copper conductors are used as earth grid conductors. This has been implemented from the beginning of power system grounding practise. The earth grid is installed for the designed lifetime of the substation which can be in excess of 30 years. The grounding system is designed to dissipate the power system fault current, or the lighting strikes to the ground for safeguarding the electrical equipment from damage. Most importantly the grounding system provides protection to the humans from the electric shock incident inside and near the substation during normal or fault conditions. For a defined prospective fault current, step and touch voltages and the rise of earth potential are kept below a safe limit. Over time, the prospective fault current may increase. The state and effectiveness of the earth grid may also change. This may occur because of a change in soil characteristics (moisture, pH, and organics), corrosion, accelerated aging from lightning and earth current flows. The encroachment of the urban built environment may also put the public closer to previously relatively isolated substation structures. In various situations these conditions can potentially lead to instances of higher than designed rise of earth potential, unsafe step and touch potential and extended rise of earth potential outside the substation due to encroaching metallic structures. As a novel solution to these problems, graphene-coated copper conductors were investigated with the aim to both increase conductor conductivity and reduce corrosion.

Graphene is found to be a single layer of carbon atoms (Figure 1). Nano coatings offer the precision of this structure at the atomic level. Different shapes of carbon-based materials can be formed from it. Since 2004 extensive research has been conducted on the graphene film deposition and its properties and it has been found that graphene has a very high charge (electrons and holes) mobility (230,000 cm^2/Vs), thermal conductivity (3000 W/mK), the highest strength (130 GPa) and the highest theoretical specific surface area (2600 m^2/g) compared to any other thin films [1]. Graphene gives a resistivity of about 1.0 cm in room temperature which is about 35 percent less than the resistivity of copper, the lowest resistivity material reported to date [2].

Despite being atomically thin, the graphene retains these properties. Its unique property is that other than graphene no other film is even poorly metallic under ambient conditions. At these dimensions, it is assumed that the graphene layers on the metal surfaces represent the most perfect over-layers known in surface science [3]. In addition to this the graphene shows no transition to the insulator state down to the temperature of liquid helium. Geim et al. reported that graphene layers are not affected (crystal defect or generation of dislocation) at an increased temperature [4]. Bunch et al. [5] have reported that the graphene thin films can be impermeable even to the smallest gas atom. Recently Raman et al. [6] reported that the graphene coating prevents electrochemical degradation. It was shown that the corrosion resistance (arithmetical sum of metal/electrolyte interface resistance and surface coating resistance pore resistance) of a graphene-coated specimen is 1.5 times higher than an uncoated copper specimen. Graphene as an anti-corrosion coating has been identified as promising in many research articles [6]–[8].

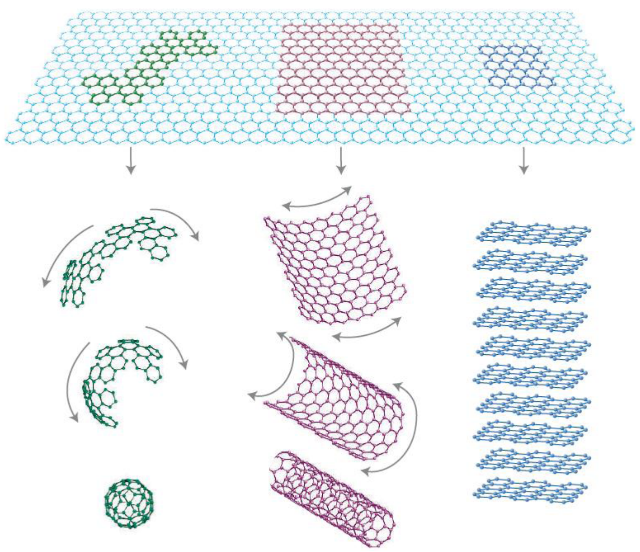

FIGURE 1. Graphene is a 2D sheet of carbon from which carbon materials of all other dimensionalities e.g. 0D buckyballs, 1D nanotubes and 3D graphite can be formed (from left to right) [4].

Graphene has a hydrophobic nature. It prevents hydrogen bonding with water [9]. Graphene is inert with respect to oxidation and other chemical reactions. Corrosion in the soil is basically an oxidation/chemical reaction. It is expected that graphene will not lose surface material in the soil. From these descriptions, graphene coating has the potential to inhibit corrosion without sacrificing conductivity.

The main contribution of this paper is the performance study of the graphene-coated copper in the grounding applications. This study aims to investigate the potential of replacing the conventional copper earth grid for AC substation grounding. Conductors are tested in both the destructive and non-destructive chemical environment to assess its corrosion susceptibility. Then a scale model test is conducted to evaluate the coated and uncoated copper bars conductivity. Bare copper and graphene-coated copper of dimension 14 cm long, and 12.7 mm diameter (which is the widely used conductor diameter) are used for all these testings. The test results show that the graphene-coated conductor corrodes less and conducts more current compared to the bare copper, and the difference between the current conduction levels is greater with increased voltage levels. Finally, the effectiveness of various earth grid topologies with different material properties across any chosen range of frequencies and applied lightning stroke waveforms is analysed with the simulation packages, CDEGS and CST.

The remainder of this paper is structured as follows: Section II provides information about graphene deposition and characterization techniques. Section III describes the electrochemical impedance study and the scale model test of the earth grid. Section IV describes the simulation studies of lightning strikes on an earth grid with two different software packages and concluding remarks are given in section V.

II. GRAPHENE DEPOSITION AND CHARACTERISATION TECHNIQUE

In this section the method of graphene deposition is described together with the subsequent analysis procedure undertaken in this study.

A. GRAPHENE DEPOSITION ON COPPER

Copper rods of diameter 12.7 millimetres were used as the substrates to investigate graphene deposition. These substrates were soaked in acetone for 5 minutes. Then ultrasonic cleaning was carried out with isopropanol. Finally the substance was rinsed with deionized water. Methane was used as the carbon source. The substrates were placed in a tube furnace and the temperature was gradually increased to 975 °C. Then H_2 gas was flown at 500 SCCM (standard cubic centimetres per minute) for 20 min at 975 °C to recover a pure metal surface. Then methane gas was introduced into the tube furnace while H_2 gas flow was maintained at the same flow rate. The graphene film growth time was 10 minutes and during this time 30 SCCM methane and 500 SCCM of H_2 gas flowed into the furnace. After completion of the graphene growth, the methane gas supply was stopped. In order to cool the tube furnace to room temperature a gas flow of 200 SCCM Ar and 100 SCCM H_2 was maintained.

B. CHARACTERISATION OF THE GRAPHENE DEPOSITION ON COPPER

Scanning electron microscopy and optical microscopy was used to observe the morphology and homogeneity of the produced graphene films. Transmission electron microscopy (TEM) and Raman spectroscopy with laser excitation wave-lengths of 532 nm was performed throughout the metal substrates surface after the chemical vapour deposition process. Theses microscopic analysis confirm the formation of graphene and characterization of the quality and the number of layers. There were non-uniform graphene layers varying from few to around 29 layers observed. The average interlayer spacing in between the graphene layers were around 0.359 nm.

III. CONVENTIONAL AND COATED CONDUCTOR TESTING

To evaluate the performance of the graphene-coated conductor samples and the uncoated samples it was tested in two test environments. These are reported in this section. Subsection III-A provides background on electrochemical impedance study of the earth grid followed by the experimental setup and test results. Subsection III-B provides background on the scale model test of the earth grid followed by the experimental procedure and the test results.

A. ELECTROCHEMICAL IMPEDANCE STUDY OF THE EARTH GRID

In this section, experimental procedures reported by Raman et al. [6] have been carried out using copper bar conductors of dimension 14 cm long and 12.7 mm radius, coated and uncoated.

The significant factors in the determination of transient response of any grounding arrangement are:

- grounding resistance - the resistance to the ground offered by each element in the grounding system
- inductance - for extensive grounds such as grids and counterpoises the transient performance is largely dependent on the self and mutual inductance of the individual element
- The ohmic resistance of the electrode
- ground capacitance.

Hence, any grounding arrangement can be represented by its distributed ground resistance (or conductance), inductance, ohmic resistance and capacitance per unit length. However, for the usual size of the electrodes used in the earth grids, the resistance is very small and is therefore neglected. The ground capacitance is assumed to be in parallel with the ground resistance (leakage conductance). The value of ground capacitance is negligible in this case. These assumptions (soil resistivity values upto 3000 ohm-metres) results in a value of time constant in the order of 0.01 to 0.1 microseconds. Subsequently, Ramamoorty et al. [10] indicated that the elements of the earth grid can be modelled with its inductance and ground conductance.

Van Westling et al. [11] described, from the viewpoint of electrochemical impedance spectroscopy, that the earth grid could be considered as an electrode of an electrochemical cell. Nyquist and Bode plots are the most common representation of an electrochemical impedance study. Bode plots are plotted in a logarithmic scale which is a function of the impedance/phase angle versus a wide range of frequency. On the other hand, Nyquist plots are plotted in linear scale which is a function of real impedance versus imaginary impedance. The frequency range is selected (figure 4) to discover when the top curve becomes asymptotic. In this case, imaginary impedance tends to zero. Hence, only the real impedance contributes to the total impedance.

1) EXPERIMENTAL SETUP

In this study, experiments were conducted in a conventional electrolytic cell with a platinum counter electrode. A saturated calomel electrode (SCE) was used as the reference electrode [7]. Anions, such as chloride, sulphite, carbonate, etc. are considered to degrade metals or alloys. But for the case under study among these anions, chloride containing electrolytes are considered the most aggressive solution [6]. The electrodes were immersed in a solution consisting of 0.5 M (0.5 molecular weight gram powder in per litre volume of solution) sodium sulphate. A second set of experiments were carried out using 0.1 M sodium chloride as the electrolyte. Exposed surface areas of the conductors to the solution were 520 mm^2. A Bio-Logic VMP 3 potentiostat was used (EC-Lab 10.17 software) to perform these experiments.

2) IMPEDANCE SPECTROSCOPY RESULTS

The results from the experimental setup are as follows: Impedance of two interfaces- metal to electrolyte, and surface coating to electrolyte, is analysed from the Nyquist plot in figure 2 and figure 3. From these figures, it can be seen that graphene-coated conductors show less resistance than the bare copper.

3) CORROSION PERFORMANCE EVALUATION

A small potential applied across the electrodes may produce a high current if the copper electrodes are corroding at a high rate [12]. This corresponds to a low polarization resistance and a high corrosion rate. This is the basis of the linear polarization measurement used to evaluate the corrosion performance of any metal/alloy. By extrapolating the Tafel lines (branches of polarization curve) to corrosion potential and determining their slope, cathodic and anodic Tafel slopes can

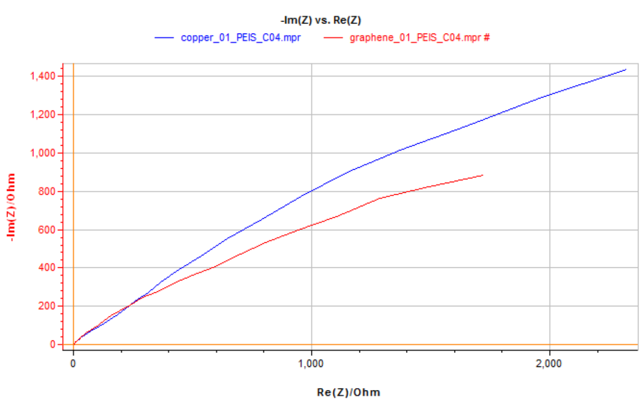

FIGURE 2. Electrochemical impedance spectroscopy of bare and graphene-coated copper conductors in 0.5 M Sodium sulphate solution.

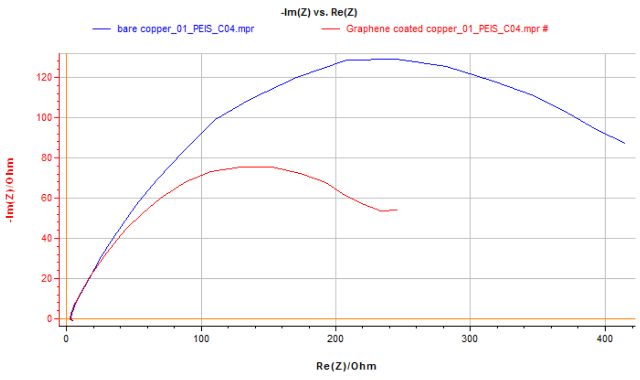

FIGURE 3. Potentio electrochemical impedance spectroscopy of bare and graphene-coated copper conductors in 0.1 M Sodium chloride solution.

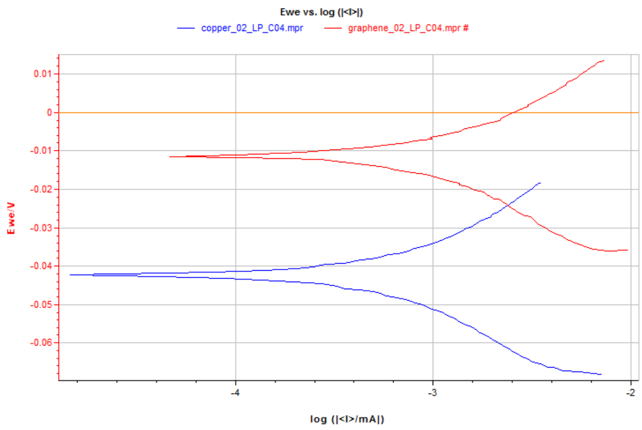

FIGURE 4. Polarization curves of the graphene-coated and uncoated copper in 0.5 M sodium sulphate solution.

be computed. Corrosion current density can be also calculated from the intersection point of the two lines (given that the anodic and the cathodicTafel lines show linear behavior) [13].

During the linear polarization, the anodic dissolution rate of any metal can be determined from the anodic current density. On the other hand, cathodic current density of the sample is estimated from the rate of oxygen reduction reaction [14]. The anodic current densities of the graphene-coated conductors were almost the same in magnitude to the uncoated specimens.

The corrosion potential, E_{corr} quantifies the intensity of corrosion susceptibility. The shift in E_{corr} in the more positive direction indicates less susceptibility to corrosion. Ecorr (i.e., the intercept of the anodic and cathodic regions of the plot) of the graphene-coated copper sample was 30 mV more positive than the uncoated copper sample in both solutions. This indicates that the graphene-coated copper will corrode less than bare copper.

From an electrochemical point of view, electrons enter the metal and metal ions diffuse into the electrolyte. Resistance across an electrode-electrolyte interface is defined as the charge transfer resistance. Electricity conduction increases as the charge transfer resistance decreases. From the experimental data of these experiments (Figure 4, 5) it suggests that the charge transfer resistance has reduced for the graphene-coated samples. This enables a facilitated path to discharge the current to ground. Overall these electrochemical studies indicate, graphene coating contributes to increased conductivity.

B. SCALE MODEL TEST OF THE EARTH GRID

The scale model test of the conductor grid was assembled to predict the performance of the earth grid system in a soil environment. The accuracy of the results obtained in the scale model tests is verified by comparing them with the data available in the literature. For the scale model tests, all the physical dimensions are scaled down using the same scaling factor. The physical dimensions are conductor diameter, conductor installation depth, and the soil resistivity. It is observed that

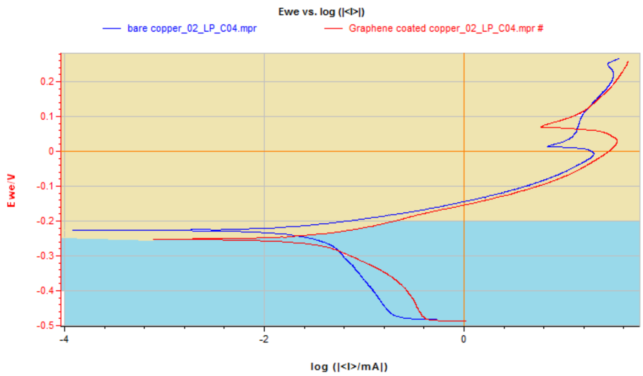

FIGURE 5. Polarization curves of the graphene-coated and uncoated copper in 0.1 M sodium chloride solution. (Light yellow indicates the anodic region and light turquoise the cathodic region of the plots.) As the intercept point of anodic and cathodic plots has shifted to the positive direction it could be reported that the graphene-coated copper conductor will be less susceptible to corrosion than the uncoated copper.

the equipotential surface profiles remain unchanged in scale model tests [15]. The following was undertaken:

The water model was a stable mix. There was flexibility to change the resistivity of the layers. The liquid models give better test results because they facilitate:

a) measurements of potentials
b) replacement and modification of the grounding models representing the earth grid conductors
c) proper contact with the conductors of the model and the dimensions of the electrolytic tank were sufficient to eliminate the boundary effect.

In the initial scale model tests, tap water was used to represent the uniform soil model. The use of a small model in the large tank generated consistent results. It enabled to test different earth grid models in various conditions and to evaluate the effects of change in different parameters to be observed. Koch introduced a method to use a scale model in an electrolytic tank to determine the earth potential rise during earth faults in 1950 [16]. Then at EcolePolytechnique a two layer laboratory model was developed which used concrete blocks to represent lower layer soil [17]. Ohio State University [18] developed a system using agar (a gelatin-like material) to represent the lower levels of soil. The results of the model tests have shown that the scale models can be utilized for parametric analysis of earth grid design and verifying computer simulations of earth grid parameters.

In these methods, the resistivity of the scale model soil layers could not be controlled precisely. In addition to this, the resistivity of the medium could not be held to a specific value for a long period. Thapar and Goyal [15] introduced a method to overcome these disadvantages. They suggested using tap water or salt water to represent both the mediums. It required an acrylic sheet to keep the two mediums separate without hampering the conduction of the electric current.

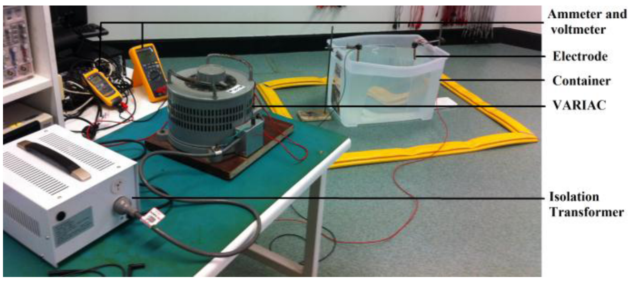

FIGURE 6. Experimental setup for scale model test of earth grid.

1) EXPERIMENTAL PROCEDURE

Two conductor rods were immersed into the water (figure 6). To maintain the same test environment for both sets of conductors, all the rods were dipped 2 cm into the water. Therefore, 916.37 mm^2 was the exposed metal surface area to the water. Water was chosen as the conducting medium for the ease of the experiment as it facilitates current conduction and is very easily sourced. The conductors were connected to the power supply. The test procedure consists of applying voltages across the two electrodes for the purpose of calculating impedance. This procedure is prescribed as part of a standard operating procedure in IEEE documentation [18]. The current was drawn from the nominated outlet; an isolating transformer was used for safety and was varied during the test with an auto transformer. The current and voltage were measured by conventional electrical measuring instruments to derive the test cell impedance. The test duration was typically around half an hour for each test.

2) TEST RESULTS

Different voltages (up to 274) volts were applied across the conductors for the copper-copper electrode system and the graphene coated copper-graphene coated copper system. The time required to apply the specific voltage and to decrease to zero was also recorded. After applying a certain voltage, current was measured. From the test results (figure 7) it can be seen that the graphene-coated copper system conducted more current than the bare copper electrode system for the same applied voltage. The conductor surfaces before and after the tests are shown in (figure 8). It appears that before the experiment the graphene-coated conductor has a shinier surface than the bare copper conductors. But after the current conduction (as well as corrosion to some extent) the graphene-coated copper conductors turned darker than the corroded bare copper conductors. Microscopic/spectroscopic tests are required in order to gain better understanding of the surface morphology of these corroded conductors. This is not reported in this paper.

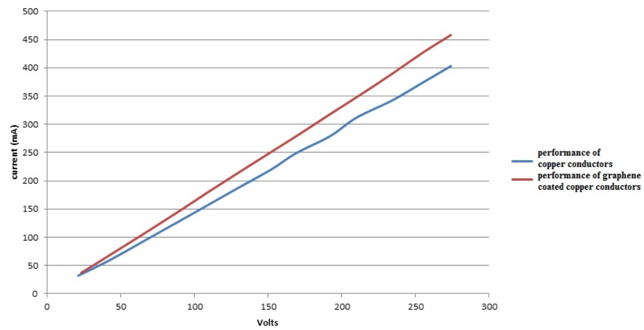

FIGURE 7. Experimental results of the scale model test of the earth grid.

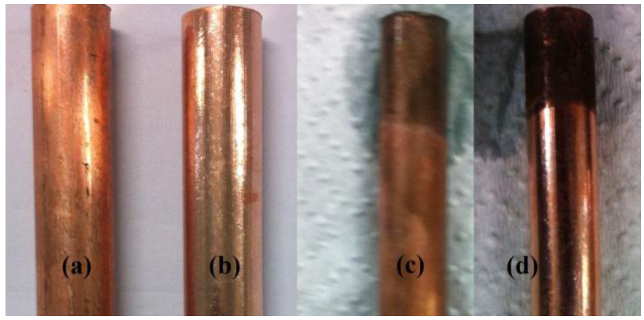

FIGURE 8. Uncoated copper conductor before (a) and after (c) I-V test, graphene-coated copper conductor before (b) and after (d) I-V test.

IV. SIMULATIONS STUDIES OF LIGHTNING STRIKES ON EARTH GRID WITH DIFFERENT SOFTWARE PACKAGES

This part of the article explores the post processing capability of simulation software packages, CDEGS [19] and CST [20]. In particular, this summary shows the visualisations that are produced for the user to assess the suitability of any proposed earth grid design and the effect of lightning strikes or conduits in the soil.

Dawalibi et al. [21] described the computational method of CDEGS as follows: in CDEGS ''field theory method'' based computational method is used to calculate the electromagnetic field and the impulse performance of any grounding system. CDEGS calculates current distributions in the earth grids and the networks of transmission lines affected by a fault current at arbitrary point using one of the following approaches [22]:

The first approach solves the electric field point matching equations in a weighted least square formulation with

IEEE Access
The journal for rapid open access publishing

linear constraints on the currents. The second approach uses a power minimization algorithm which is more applicable for calculation in the low-frequency range. For the calculations in the low-frequency domain, Faradays law is being utilized by this software package. The electromagnetic fields are then calculated based on the method of moments and the numerical integration of Sommerfeld integrals [23]. The response of the conductors to the each component of Hertz vector potential is translated into line integrals. A conductor network is segmented into short elements of the tangential oscillating dipole to calculate path integral of electromagnetic quantities [23], [24]. All the above frequency domain calculations are then translated to the time domain quantities by inverse Fourier transformation. The overall chronological evolution of the electric or magnetic field distribution along a calculation domain can be obtained by calculating the inverse Fourier transformation at each point in that domain.

On the other hand in CST STUDIO SUITE, after setting up the model geometrically and assigning the appropriate power sources and boundary conditions, the model has to be translated into a computation accessible format. For this purpose, the calculation domain has to be subdivided into small cells, on which Maxwell's Equations are to be solved. Numerical methods transform the continuous integral or differential equations of Maxwell into an approximate discrete formulation that requires either the inversion of a large matrix or an iterative procedure [25]. The computation approach used to produce the results is based on a hybrid of the circuit theory and the field theory named as the hybrid theory. CST STUDIO SUITE offers a variety of meshes and algorithms. The mesh influences the accuracy and the speed of the simulation. For our model, Hexahedral TLM meshing was used because it facilitates lightning studies and offers a very efficient octree based meshing algorithm which drastically reduces the overall cell count. The algorithm for the generation of hexahedral element meshes is based on two basic steps. Firstly an initial mesh of cubes is generated in the interior of the volume. Subsequently, the boundary region is meshed by creating a structure on the contour that is isomorphic to the surface of the initial mesh [26].

In this section, lightning strikes have been selected for the fault simulation using the software packages CDEGS and CST. Lightning strikes will generate a high fault current, and this will facilitate a comparison between CDEGS and CST. To reduce the computation time, a simplified model of a grounding system was used to obtain the electric field, magnetic field and current densities across various test points. The model consisted of a copper rod (the ground conductor) with a radius of 6.25 millimetres and 0.5 metres length and was installed at a depth of 0.5 metres in an uniform soil with a 100 ohm-metres resistivity, a relative permittivity of 1 and relative permeability of 1.

The lightning surge current considered in this study for both CDEGS and CST is defined by the following double exponential type function. The lightning surge was fed to the ground conductor with a copper wire of 6.25 millimetres radius and 0.5 metres length.

$$I(t) = I_m(e^{-\alpha t} - e^{-\beta t}) \tag{1}$$

where, $I_m = 30\,\text{kA}$, $\alpha = 1.4 \times 10^4\ \text{s}^{-1}$ and $\beta = 6 \times 10^6\ \text{s}^{-1}$. This wave is characterized by a rise time of 1s and a half value time of 50s, which are typical values for lightning strokes (MIL-STD-464, DO160).

In CDEGS the Fourier transform of the lightning strike current signal results in the following frequency locations where the electromagnetic field distribution in the field is calculated: 0, 10 kHz, 20 kHz, 30 kHz, 40 kHz, 50 kHz, 60 kHz, 70 kHz, 90 kHz, 110 kHz, 140 kHz, 250 kHz, 360 kHz, 540 kHz, 720 kHz, 1.08 MHz, 1.44 MHz, 1.8 MHz, 2.16 MHz, 2.52 MHz and 2.56 MHz. Figure 9 shows the electric field distribution at 50 Hz and 1 MHz which were the user selected frequency for study. It was observed that the dissipated current in the earth conductor does not flow from the conductor end surface but dissipates down the end of the earthing conductor.

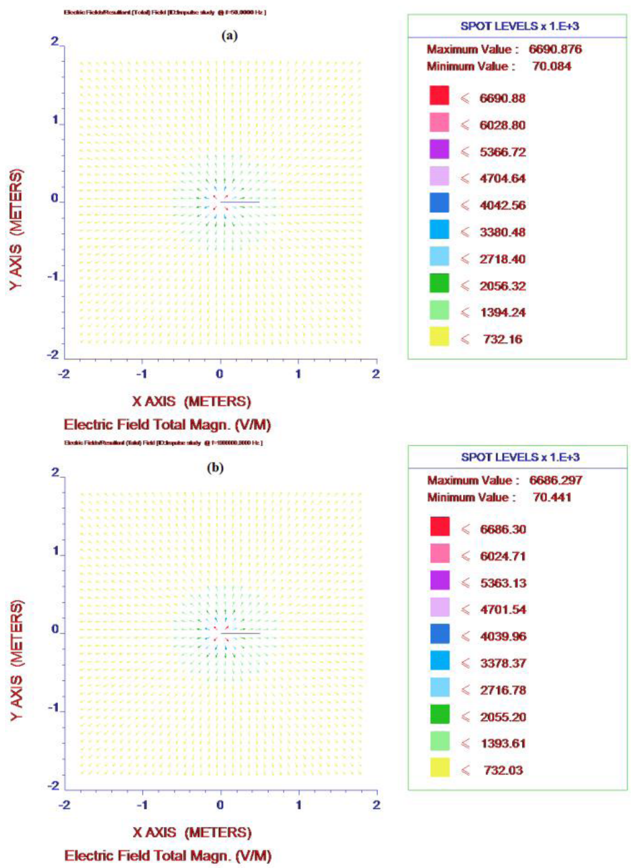

FIGURE 9. Electric field distribution at earth surface at a lightning incident at 50 Hz frequency (a) and at 1 MHz frequency (b).

Apart from the previously stated results from CDEGS, CST microwave suite has additional benefits such as finer resolution for electromagnetic field distribution

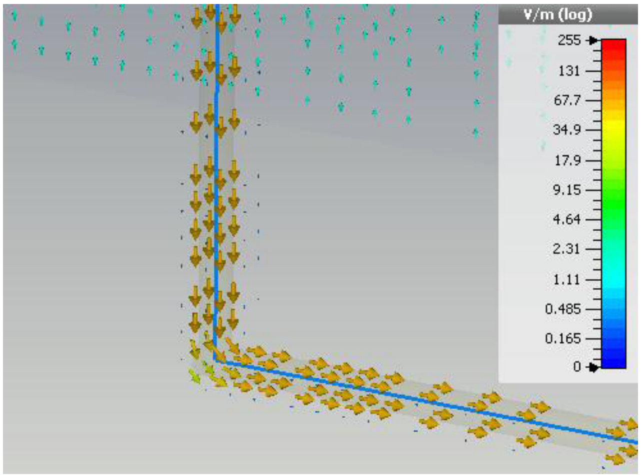

FIGURE 10. Electric field distribution in the model at a lightning incident at 50 Hz frequency at a depth profile (detailed picture of E field as shown in figure 9 with a horizontal scale of the conductor = 0.5 metres).

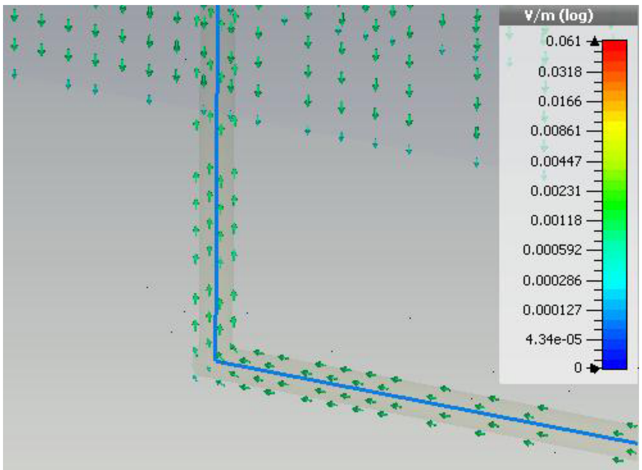

FIGURE 11. Electric field distribution in the model at a lightning incident at 1 MHz frequency at a depth profile (detailed picture of E field as shown in figure 9 with a horizontal scale of the conductor = 0.5 metres).

(Figure 10 and 11). Figure 12 indicates the input power's frequency spectrum of the applied lightning impulse.

The response of the buried earth conductor to the applied lightning stroke is shown in figure 13, 14 and 15. In this case,

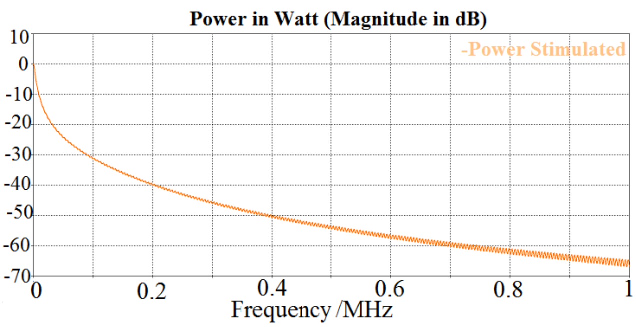

FIGURE 12. Input power's frequency spectrum of lightning impulse.

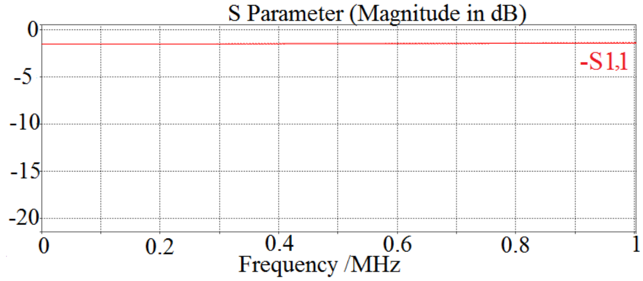

FIGURE 13. S parameter result through the conductor (normalized to 50 Ohms input impedance).

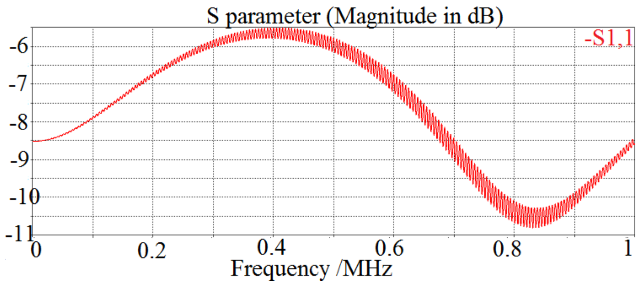

FIGURE 14. S parameter result through the conductor (normalized to 300 Ohms input impedance).

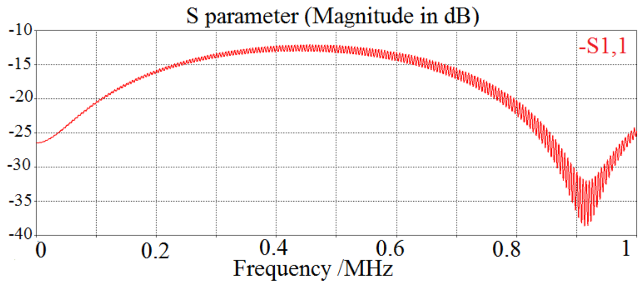

FIGURE 15. S parameter result through the conductor (normalized to 600 Ohms input impedance).

the reflection scattering parameter S_{11} is used as the measured quantity which gives an indication of the impedance matching of the lightning stroke to the earth grid system. In figures 13, 14 and 15 the input impedance is set at 50 Ohms, 300 Ohms and 600 Ohms respectively. The consequent S_{11} response indicates that 600 Ohms is the best impedance match from 50Hz to 1MHz. In this way, CST can provide a clear indication of the effectiveness of any earth grid topology across any chosen range of frequencies and applied lightning stroke waveforms.

During the preparation of this paper, an earth grid monitoring unit was being designed to be installed at a 275 kV substation. One of the parameters measured by this unit will be the effective earth grid resistance following a lightning stoke incident. This will provide data over the long term of the effectiveness of the earth grid when struck by lightning as well as an indication of the effectiveness of the earth grids impedance matching to the applied lightning waveform.

The material library in CST allows the user to define material properties and earth grid conductor composite structures. This allows the user potentially to include a composite graphene/copper conductor for analysis. At present, the complete material analysis of the significant thickness of graphene on copper is yet to be synthesized and measured. Once this data available the effect of the composite conductor can be analysed for its impulse response as described above.

V. CONCLUSION

This paper presents the performance study of the graphene-coated copper in the grounding applications. From the electrochemical impedance spectroscopy, it was observed that the graphene-coated copper is less susceptible to corrosion than the uncoated copper. Conductors were tested in both the destructive and a non-destructive chemical environment, and the anodic and the cathodic current densities were compared to get an insight of the graphene-coated copper's performance in any kind of soil. With the control over the deposition process resulting in more uniform deposition and coverage, we could expect improved corrosion control. Scale model tests were conducted in a water medium setup to evaluate the conductivity and the grounding behaviours with the graphene-coated samples. The graphene-coated copper system conducted more current than the bare copper electrode system for the same applied voltage. It is also worth noting that the difference between the current conduction levels is greater with increased voltage levels. There is potential to coat a less expensive metal than copper with graphene and achieve the conductivity and corrosion control measured in this work. Such an application using the less expensive material would allow significant saving in the cost of large earth grids. The final section of this paper discusses the different attributes of the simulation packages CDEGS and CST when assessing lightning strike performance of an earth grid.

ACKNOWLEDGMENT

The authors also acknowledge the support of the Central Analytical Research Facility (CARF), QUT during the graphene deposition and characterization process of the experiments.

REFERENCES

[1] V. Singh, D. Joung, L. Zhai, S. Das, S. I. Khondaker, and S. Seal, "Graphene based materials: Past, present and future," *Progr. Mater. Sci.*, vol. 56, no. 8, pp. 1178–1271, 2011.
[2] (Mar. 24, 2015). *Electrons Can Travel Over 100 Times Faster in Graphene Than in Silicon, Physicists Show*. [Online]. Available: http://www.sciencedaily.com/releases/2008/03/080324094514.htm
[3] J. Wintterlin and M.-L. Bocquet, "Graphene on metal surfaces," *Surf. Sci.*, vol. 603, nos. 10–12, pp. 1841–1852, 2009.
[4] A. K. Geim and K. S. Novoselov, "The rise of graphene," *Nature Mater.*, vol. 6, no. 3, pp. 183–191, 2007.
[5] J. S. Bunch *et al.*, "Impermeable atomic membranes from graphene sheets," *Nano Lett.*, vol. 8, no. 8, pp. 2458–2462, 2008.
[6] R. K. S. Raman *et al.*, "Protecting copper from electrochemical degradation by graphene coating," *Carbon*, vol. 50, no. 11, pp. 4040–4045, 2012.
[7] N. T. Kirkland, T. Schiller, N. Medhekar, and N. Birbilis, "Exploring graphene as a corrosion protection barrier," *Corrosion Sci.*, vol. 56, pp. 1–4, Mar. 2012.
[8] L. Cardenas *et al.*, "Reduced graphene oxide growth on 316L stainless steel for medical applications," *Nanoscale*, vol. 6, no. 15, pp. 8664–8670, 2014.
[9] O. Leenaerts, B. Partoens, and F. M. Peeters, "Water on graphene: Hydrophobicity and dipole moment using density functional theory," *Phys. Rev. B*, vol. 79, no. 23, p. 235440, 2009.
[10] M. Ramamoorty, M. M. B. Narayanan, S. Parameswaran, and D. Mukhedkar, "Transient performance of grounding grids," *IEEE Trans. Power Del.*, vol. 4, no. 4, pp. 2053–2059, Oct. 1989.
[11] E. P. M. van Westing, G. M. Ferrari, F. M. Geenen, and J. H. W. de Wit, "*In situ* determination of the loss of adhesion of barrier epoxy coatings using electrochemical impedance spectroscopy," *Progr. Organic Coat.*, vol. 23, no. 1, pp. 89–103, 1993.
[12] *Caproco Linear Polarization Resistance (LPR) General Information*, Caproco, Edmonton, AB, Canada, Dec. 2014.
[13] A. Kosari *et al.*, "Theoretical and electrochemical assessment of inhibitive behavior of some thiophenol derivatives on mild steel in HCl," *Corrosion Sci.*, vol. 53, no. 10, pp. 3058–3067, 2011.
[14] G. Kear, B. D. Barker, and F. C. Walsh, "Electrochemical corrosion of unalloyed copper in chloride media—A critical review," *Corrosion Sci.*, vol. 46, no. 1, pp. 109–135, 2004.
[15] B. Thapar and S. L. Goyal, "Scale model studies of grounding grids in non-uniform soils," *IEEE Trans. Power Del.*, vol. 2, no. 4, pp. 1060–1066, Oct. 1987.
[16] W. Koch, "Grounding methods for high-voltage stations with grounded neutrals," *Elektrotechnische Zeitschrift*, vol. 71, no. 4, pp. 89–91, 1950.
[17] *IEEE Guide for Safety in AC Substation Grounding*, IEEE Standard 80-2000, 2000, pp. 1–192.
[18] J. Sverak, C. Booraem, and D. Kasten, "Post-design analysis and scale model tests for a two grid earthing system serving the 345 kV GIS facilities at Seabrook power plant," in *Proc. CIGRE Symp. High Currents Power Syst. Under Normal, Emergency Fault Conditions*, 1985, pp. 6–410.
[19] *Current Distribution Electromagnetic Interference Grounding and Soil Structure Analysis*, Safe Engineering Services and Technologies Ltd., Laval, QC, Canada, 2015.
[20] *Computer Simulation Technology AG*, CST, Darmstadt, Germany, 2015.
[21] F. P. Dawalibi, W. Xiong, and J. Ma, "Transient performance of substation structures and associated grounding systems," *IEEE Trans. Ind. Appl.*, vol. 31, no. 3, pp. 520–527, May/Jun. 1995.
[22] A. Selby and F. Dawalibi, "Determination of current distribution in energized conductors for the computation of electromagnetic fields," *IEEE Trans. Power Del.*, vol. 9, no. 2, pp. 1069–1078, Apr. 1994.
[23] F. Dawalibi and A. Selby, "Electromagnetic fields of energized conductors," *IEEE Trans. Power Del.*, vol. 8, no. 3, pp. 1275–1284, Jul. 1993.
[24] L. Grcev and F. Dawalibi, "An electromagnetic model for transients in grounding systems," *IEEE Trans. Power Del.*, vol. 5, no. 4, pp. 1773–1781, Oct. 1990.
[25] D. G. Swanson and W. J. Hoefer, *Microwave Circuit Modeling Using Electromagnetic Field Simulation*. Norwood, MA, USA: Artech House, 2003.
[26] R. Schneiders, "A grid-based algorithm for the generation of hexahedral element meshes," *Eng. Comput.*, vol. 12, nos. 3–4, pp. 168–177, 1996.

AMIT JYOTI DATTA received the B.Sc. degree in electrical and electronic engineering from the Chittagong University of Engineering and Technology, Bangladesh, in 2012. He is currently pursuing the master's degree with the Queensland University of Technology, Australia. He worked in different projects with Interchain project consultants. He has worked with Powerlink Queensland, Australia, in an earthing project.

RICHARD TAYLOR (M'09) received the B.E. and master's degrees in electrical engineering from Canterbury University, NZ, in 1977 and 1979, respectively, and the Ph.D. degree from The University of Queensland, Australia, in 2007.

He was a Communications Project Engineer with NZ Electricity from 1980 to 1982, and a Project and Protection Engineer with SWQEB, QLD, Australia, from 1980 to 1984. From 1986 to 2010, he founded three technology-based companies, which developed device applications using novel ceramics and superconductors for the power and communications industries.

He joined the Queensland University of Technology as an Adjunct Professor in 2010, jointly with the School of Electrical Engineering and Computer Science, and The Institute of Future Environments. As a CIGRE Member, he serves on WG D1.38 for common characteristics and emerging test techniques for high temperature superconducting power equipment.

His areas of interest include applications of superconductivity, novel ceramics, and high conductivity coatings, such as graphene.

GEOFFREY WILL is currently an Associate Professor with the Queensland University of Technology (QUT), Brisbane, and is the Discipline Leader for Energy and Process Engineering. He leads the Corrosion Consulting and Research Group, QUT. His current research involves protective coating degradation, modeling of polarization curves, and sensors for corrosion monitoring.

GERARD LEDWICH (SM'89) received the Ph.D. degree in electrical engineering from the University of Newcastle, Callaghan, NSW, Australia, in 1976. He has been a Chair Professor of Electrical Power Engineering with the Queensland University of Technology, Brisbane, QLD, Australia, since 1998, and was the Head of the Electrical Engineering Department with the University of Newcastle from 1997 to 1998. From 1976 to 1994, he was with The University of Queensland, Brisbane. His current research interests include the areas of power systems, power electronics, and controls. He is a fellow of the Institute of Engineers in Australia.